Spin-flip Raman scattering of the resident electron in singly charged (In,Ga)As/GaAs quantum dot ensembles

J. Debus,[1,*] V. F. Sapega,[2,3] D. Dunker,[1] D. R. Yakovlev,[1,2] D. Reuter,[4] A. D. Wieck,[5] and M. Bayer[1,2]

[1]*Experimentelle Physik 2, Technische Universität Dortmund, 44227 Dortmund, Germany*

[2]*Ioffe Physical-Technical Institute, Russian Academy of Sciences, 194021 St. Petersburg, Russia*

[3]*Spin Optics Laboratory, St. Petersburg State University, 198504 St. Petersburg, Russia*

[4]*Department Physik, Universität Paderborn, 33098 Paderborn, Germany*

[5]*Angewandte Festkörperphysik, Ruhr-Universität Bochum, 44780 Bochum, Germany*

(Received 22 September 2014; revised manuscript received 10 November 2014; published 1 December 2014)

Highly efficient spin-flip Raman scattering of the resident electron spin is found in singly charged (In,Ga)As/GaAs quantum dots. The applied magnetic field induces a symmetry reduction for the negatively charged exciton, which serves as intermediate scattering state, thus making the spin-flip Raman scattering of the resident electron allowed. Electron-electron exchange interaction mediates the electron spin-flip. Above a threshold magnetic field that depends on the dot size and experiment geometry, the efficiency of the scattering cross section is spectrally shifted with increasing field. This shift, which follows the electron cyclotron energy, is assigned to a hybridization of s-shell singlet and p-shell triplet states of the negatively charged exciton.

DOI: 10.1103/PhysRevB.90.235404 PACS number(s): 75.75.−c, 78.67.Hc, 73.21.La, 81.07.Ta

Semiconductor quantum dots (QDs) have aroused remarkable interests in most diverse scientific fields. In particular, they open new opportunities in spin-electronics and quantum information technologies [1–3]. A major possibility of implementing solid-state quantum information applications is offered by carrier spins in ensembles of QDs [4]. In order to realize such applications a robust spin coherence is a major requirement. In this respect, excitons, while being considered, are less prospective due to their short lifetime than resident electrons as being present in singly charged QDs [5,6]. As example, for preparation and read-out of spin coherence at high frequency, optical methods based on ultrashort laser pulses in subpicosecond range are used [7]. These pulses generate spin oriented electron-hole pairs in QDs which already possess a resident electron. The generation of spin coherence for the resident electron is mediated by the charged exciton complex (negatively charged trion). Hereby, not only the ground singlet state of the trion but also its excited states can be involved [8,9]. Therefore, the energy and spin structure of this exciton-electron complex and its spin dynamics need to be understood in great depth. Various optical methods have already been exploited for such studies, among them high-resolution spectroscopy showing its strength for single-dot studies and time-resolved pump&probe techniques of Faraday rotation mainly used for ensemble measurements [6,10–12].

Resonant spin-flip Raman scattering (SFRS) of resident spins in quantum dots subjected to an external magnetic field is a tool for their coherent manipulation. SFRS is also a powerful experimental technique that delivers information on Zeeman splittings of carriers and excitons and on the selection rules, which give insight into the spin structure of exciton complexes, their symmetries and spin interactions [13]. This technique is demanding in experimental realization, since the spin-flip signals are needed to be measured in the immediate vicinity of the laser line being separated from it by few hundreds of μeV only. Most probably because of that, despite the comprehensive information that can be gathered by the SFRS, there are only rare examples of its use for investigation of self-assembled QDs [14,15]. Open questions until now are related to the cross section of single spin-flip Raman scattering of a confined carrier and the symmetry requirements in QD structures, namely the magnetic field configuration, for the allowance of a respective process.

In this paper, the electron spin-flip scattering under resonant excitation is studied in ensembles of singly charged (In,Ga)As/GaAs QDs. The analysis of the selection rules for the spin-flip line measured in different configurations of external magnetic fields highlights the role of the charged exciton complex as an intermediate scattering state for the spin-flip of the resident electron. Isotropic electron-electron exchange is revealed as the main interaction mechanism. We further show that the spin-flip process becomes possible by magnetic-field-induced symmetry reduction. In that context, the scattering efficiency for the negative trion is compared with that for the neutral exciton, where the electron spin is scattered by an acoustic phonon. In slightly oblique magnetic field geometry and above a threshold field strength, a considerable shift of the maximum of the SFRS efficiency is found in weakly confining QDs. It is attributed to the mixing of s-shell singlet and p-shell triplet trion states and their repulsion which is defined by the electron cyclotron energy.

Three samples with self-assembled (In,Ga)As/GaAs QDs were fabricated from one structure grown by molecular-beam epitaxy on (001)-oriented GaAs substrate. They contain 20 layers of lens-shaped QDs with a density of 10^{10} dots per cm^2. A charging by about one electron per dot was provided by modulation doping with Si donors 20 nm below each QD layer. After growth, the samples were annealed at different temperatures of 900 °C (#1), 945 °C (#2), and 980 °C (#3) leading to different QD sizes and composition profiles [16]. Detailed optical studies of such QDs can be found in Ref. [17]. A reference sample with undoped (In,Ga)As/GaAs QDs, which were annealed at 960 °C and showed a photoluminescence (PL) spectrum with maximum at 1.401 eV, was also studied; see details on the sample in Ref. [18]. For the

*Corresponding author: joerg.debus@tu-dortmund.de

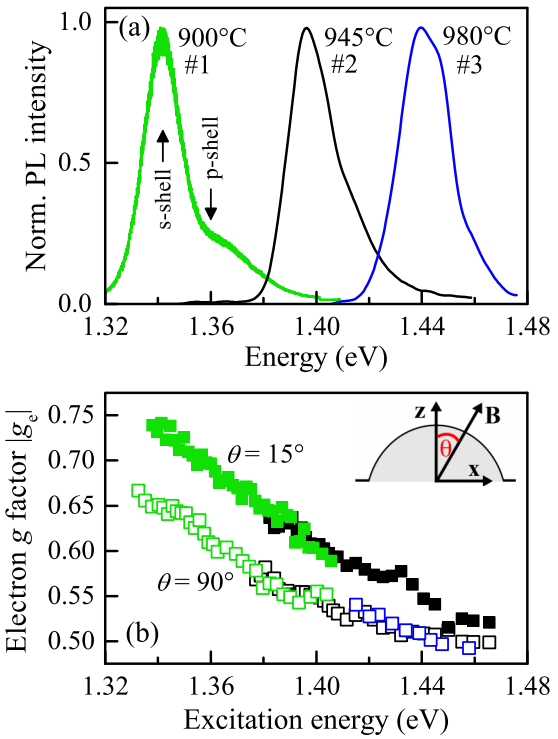

FIG. 1. (Color online) (a) PL spectra of the singly charged (In,Ga)As/GaAs QD samples excited at an energy of 1.54 eV above the band gap of the wetting layer, excitation density is 0.5 W/cm^2; $T = 6$ K, and $B = 0$ T. The arrows mark the s- and p-shell peaks for sample #1. (b) Dispersion of electron g factor across the QD ensembles of studied samples at $B = 8$ T is demonstrated for $\theta = 15°$ and 90°. Symbol colors correspond to that for the PL spectra shown in (a). The inset illustrates the tilting angle θ between the QD growth z-axis and magnetic field direction **B**.

SFRS experiments performed at a temperature of $T = 6$ K, the samples were attached strain free to a rotation holder and were exposed to external magnetic fields B up to 10 T. The QDs were excited by a tunable continuous-wave Ti:Sapphire laser with a typical power density of 5 W/cm^2. The scattered light was analyzed by a triple spectrometer equipped with a liquid-nitrogen cooled charge-coupled-device camera or a cooled GaAs photomultiplier. The backscattered SFRS experiments were performed in the Faraday ($\theta = 0°$) and Voigt ($\theta = 90°$) geometries as well as in tilted geometries, where the magnetic field **B** and QD growth axis **z** enclosed an angle $0° < \theta < 90°$ within the xz plane, as illustrated in the inset of Fig. 1(b).

Photoluminescence spectra of the singly charged (In,Ga)As/GaAs QDs are shown in Fig. 1(a). PL peaks of each QD ensemble are attributed to s-shell trions, and high-energy shoulders belong to p-shell trions; both are marked by arrows exemplarily for sample #1. The s-shell peak energies for the samples #1, #2, and #3 are 1.341, 1.396, and 1.439 eV, respectively. Diffusion of gallium atoms from the barrier material into the QDs during the annealing increases the band-gap energy which results in the high-energy shift of the PL bands. The QD size was also increased thus reducing the role of carrier quantum confinement within the plane of the annealed QDs.

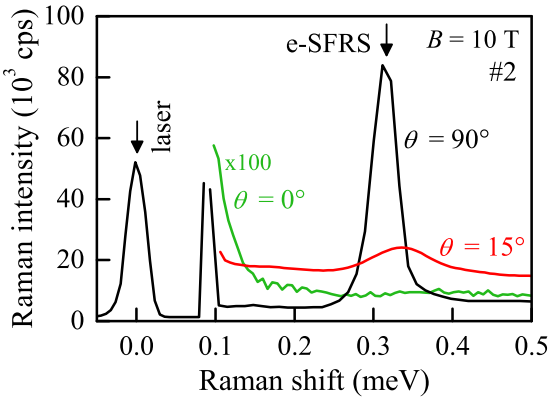

FIG. 2. (Color online) SFRS Stokes spectra of sample #2 for Faraday, tilted ($\theta = 15°$), and Voigt geometries in crossed linear polarization, excited at 1.396 eV; $T = 6$ K, $B = 10$ T.

An SFRS spectrum consists of lines which shift from the laser excitation energy, taken as zero value of the Raman shift, and usually describes the Zeeman splitting of spin states. As an example, in Fig. 2 SFRS spectra for sample #2 are shown for the excitation energy 1.396 eV corresponding to the PL maximum. Spectra of the other samples are similar to these for sample #2. One can see in Fig. 2 a strong electron-SFRS line in the Voigt geometry at $B = 10$ T measured in crossed linear polarizations. The Raman shift of this line $\Delta E_{SF} = 0.31$ meV corresponds to the in-plane electron (e) g factor $|g_e^{\perp}| = 0.54$. The latter is calculated by $\Delta E_{SF} = |g_e^{\perp}|\mu_B B$, where μ_B is the Bohr magneton, and agrees well with pump&probe measurements for (In,Ga)As/GaAs QDs [17,19].

The spectral dependence of the electron g factor over a wide energy range resulting from probing the e-SFRS in all three samples is given in Fig. 1(b). One clearly observes that the electron g factor smoothly varies with energy, not only for a single sample, but also the data for the different samples smoothly connect to each other. This underlines previous studies showing that the electron g factor is mostly determined by the band gap [20]. The in-plane value $|g_e^{\perp}|$ varies from 0.67 at 1.33 eV down to 0.50 at 1.47 eV, while the quasilongitudinal $|g_e|$ at $\theta = 15°$ follows it with an offset changing from 0.08 to 0.02. A weak anisotropy is characteristic of the electron g factor in QDs, in contrast to the strong anisotropy of the heavy-hole and exciton g factors [19].

In the Faraday geometry an SFRS signal is absent; only a PL background is detected, see Fig. 2. An e-SFRS line appears, as soon as the magnetic field is tilted relative to the z axis, as seen by the red curve in Fig. 2 for the rather small tilting angle of $\theta = 15°$. Since the QDs have, to a good approximation, rotational symmetry about their growth axis, their symmetry can be described by the irreducible representation D_{2d} which is comparable to that of quantum wells. Accordingly, the e-SFRS becomes allowed in tilted geometries, where the in-plane component of the magnetic field induces a mixing of the electron spin basis eigenstates [13,15,21]. The maximum possible symmetry breaking by the applied field is achieved in Voigt geometry thus explaining the highest e-SFRS line intensity. In the following, the SFRS mechanisms will be discussed in detail.

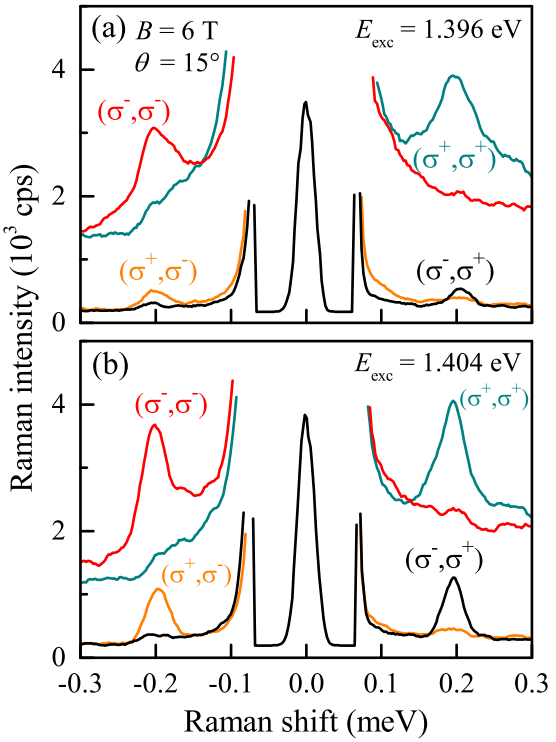

FIG. 3. (Color online) Circularly cross- and copolarized SFRS spectra of sample #2 for the excitation energy of (a) 1.396 eV and (b) 1.404 eV; $\theta = 15^\circ$, $B = 6$ T, and $T = 6$ K.

Let us now discuss the exact Faraday case in dependence on the circular polarizations of the incident and scattered light. We assume for the beginning that the valence-band ground state has heavy-hole character, despite that the admixture of light-hole is well established for the QDs studied, as evidenced by the nonzero heavy-hole in-plane g factor [19]. By using σ^+ polarized light, an electron-hole pair with electron spin opposite to the optical axis ($s_z = -1/2$), in the following denoted by $|\downarrow\rangle$, and a hole with total angular momentum $+3/2$, denoted by $|\Uparrow\rangle$, can be excited. This excitation can take place only if the resident electron spin has a component pointing upward, $|\uparrow\rangle$, otherwise it is blocked by the Pauli exclusion principle. The two electron spins then form a singlet state, so that spin flips are not possible. Indeed, we do not find indications for an SFRS process at $\theta = 0^\circ$ in the Raman spectrum recorded at $B = 10$ T, shown in Fig. 2. In principle, the heavy-hole (hh) may also flip its spin, for which we find, however, no evidence in the experiment, independent of the field configuration.

Information on the spin-flip Raman mechanism is provided by the fact that for close-to-Faraday configurations the e-SFRS line is mostly observed in cocircular polarization, i.e., the backscattered light has dominantly the same circular polarization as the incident light, as one can clearly see in Fig. 3(a). Backscattering with countercircular polarization also occurs, but its intensity is considerably reduced. In tilted magnetic field, the spin state of the resident electron can be written as $\alpha|\uparrow\rangle + \beta|\downarrow\rangle$ with $|\alpha|^2 + |\beta|^2 = 1$, using the spin basis eigenstates along the QD growth direction. The mixing coefficients depend on the tilting angle θ, and we assume that $|\alpha| > |\beta|$ for $\theta < 45^\circ$. With σ^+ polarized light only the first component in the superposition state can be excited to a trion resulting in $\alpha|\Uparrow\downarrow\uparrow\rangle + \beta|\downarrow\rangle$. A spin-flip can then occur in the second component, so that the intermediate state reads $\alpha|\Uparrow\uparrow\downarrow\rangle + \beta|\uparrow\rangle$. The spin scattering of the resident electron is mediated by isotropic exchange interaction with the photo-excited electron. Finally, the light is scattered back, and when the hole spin has remained unaffected, this light has obviously the same polarization and the resident spin has become oriented.

This scenario explains the observation of the e-SFRS with strong intensity in cocircular polarization, but does not explain the observation of a resonance - despite being weaker - in the countercircular polarizations (σ^-,σ^+) and (σ^+,σ^-) for the Stokes and, respectively, anti-Stokes scattering [22], as shown in Fig. 3(a). For such a process the hole spin has to become reversed. If this would occur solely in the trion component through acoustic phonon interaction, one would observe a hole spin-flip, which is not the case. We suggest that such a hole spin-flip is initiated by the anisotropic exchange interaction between electron and hole which is proportional to the product of the electron spin times the third power of the hole (h) angular momentum, $\mathbf{S}_e \cdot \mathbf{J}_h^3$. This interaction couples the hole spin in the trion component and the nonexcited electron spin, so that the superposition state after the flip-flop is given by $\alpha|\Downarrow\downarrow\uparrow\rangle + \beta|\uparrow\rangle$. The scattered light then has σ^- polarization, and the final state is the one of a reversed electron spin, $\alpha|\downarrow\rangle + \beta|\uparrow\rangle$, compared to the initial state. Moreover, the light-hole contribution facilitates the action of the anisotropic electron-hole exchange. By comparing the cross-polarized SFRS line intensities in the Stokes and anti-Stokes regimes in Figs. 3(a) and 3(b), one can clearly see that these intensities are larger at higher excitation energy. We propose that at higher energies the light-hole states are more strongly admixed to the heavy-hole states; hence, the spin-flip process leading to scattered light with reversed circular polarization becomes more probable.

In the reference undoped QDs an e-SFRS line is not found neither for Faraday geometry nor tilted geometry with $\theta = 15^\circ$, as depicted for 10 T in Fig. 4(a). In the Voigt geometry an e-SFRS line is observed; however, its intensity is about three orders of magnitude weaker than that of the corresponding e-SFRS process for the singly charged dots. The Raman shift $\Delta E_{SF} = 0.32$ meV corresponds to the transverse electron g factor of about 0.55 that is in agreement with previous results [19,23]. The linear magnetic field dependence of the electron Raman shift (squares) is shown in Fig. 4(b). A further SFRS line is observed in Voigt geometry with $\Delta E_{SF} = 0.25$ meV which corresponds to the absolute transverse g factor of 0.43. It is similar to that of the neutral exciton, see Ref. [19]. Moreover, the magnetic field dependence of the Raman shift of this line, measured at $\theta = 15^\circ$ [see exemplary spectrum for 10 T in Fig. 4(a)], demonstrates a zero-field offset of about 0.08 meV by linearly extrapolating the data points (circles), shown in Fig. 4(b). This offset can be assigned to the exciton exchange energy [19], which defines the splitting between the bright and dark exciton states in the neutral exciton [24]. Both the Raman shift values as well as the zero-field offset evidence that this SFRS line belongs to the neutral exciton (X). Thus, we can conclude that in the reference undoped dots the e-SFRS is performed within the X complex.

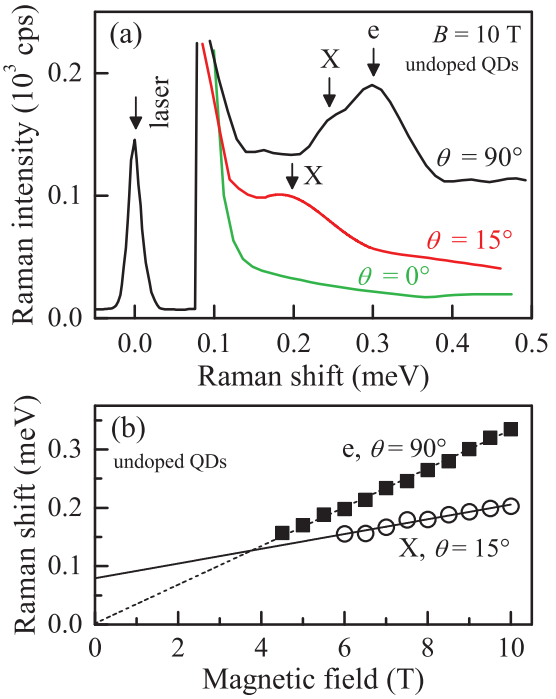

FIG. 4. (Color online) (a) SFRS Stokes spectra of undoped (In,Ga)As/GaAs QDs for different tilt angles θ. The spectra were measured at the excitation energy of 1.384 eV; $T = 6$ K, $B = 10$ T. (b) Magnetic field dependences of the electron and exciton Raman shifts in the undoped QDs.

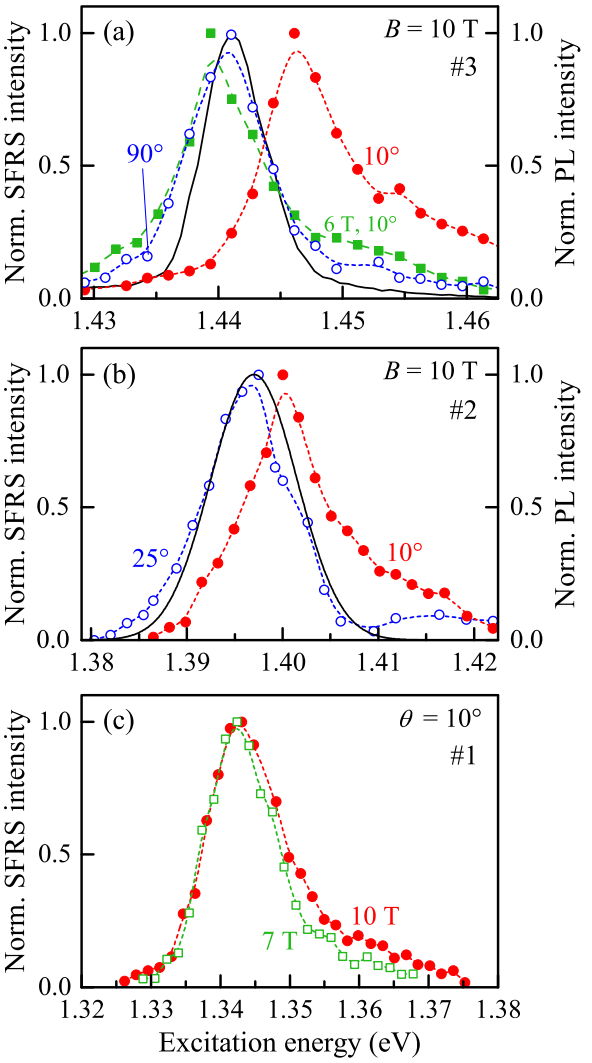

FIG. 5. (Color online) (a) and (b) SFRS resonance profiles at $B = 10$ T for samples #3 and #2, the tilting angle varies. The PL (black solid line) is shown for 10 T and 10°. In (a) the SFRS resonance profile at $\theta = 10°$ and 6 T is additionally demonstrated (green solid squares). In (c) the resonance profiles for sample #1 measured at 7 and 10 T are shown, $\theta = 10°$. Dashed lines are guides for the eye.

The mechanism of the electron spin-flip differs for the neutral and negatively charged exciton. While the spin-flip is caused by electron-electron exchange interaction in the negative trion, in the neutral exciton the electron spin is scattered by an acoustic phonon [15]. In contrast to the negative trion, in the exciton the SFRS process competes with the electron-hole exchange, which stabilizes the electron spin along the QD growth axis [25]. In Voigt geometry at the applied magnetic field of 10 T, the Zeeman splitting of the electron spin states is approximately three times larger than the electron-hole exchange energy. Accordingly, the probability of an electron spin-flip is increased. We propose that it is mediated by an acoustic phonon, while the definite type of the electron-phonon interaction cannot be determined; it may be attributed to deformation-potential, piezoelectric coupling, or interface motion [26,27]. Note that in the anti-Stokes regime the e-SFRS line is also observed (not shown here), its intensity is about twice smaller than that of the Stokes line. By considering the Bose-Einstein distribution function for the phonon statistics [28], the intensity ratio demonstrates that the electron spin temperature corresponds to the sample temperature of 6 K.

Beside the strong symmetry dependence of the e-SFRS and the spin rearrangement by SFRS in the singly charged QDs, we need to discuss the efficiency of the interaction mechanism in detail. Hence, we now turn to the SFRS resonance profile which is the dependence of the e-SFRS line intensity on the excitation energy tuning across the inhomogeneous distribution of transition energies for the QD ensemble. The SFRS resonance profiles of all three studied QD samples are shown in Figs. 5(a)–5(c) where the symbols connected by dashed lines indicate the SFRS intensities while the black solid lines give the PL spectra. In the following, we compare the energies of the PL maximum with the energies at which the SFRS efficiency is maximum. Independent of the magnetic field strength in Voigt geometry, the SFRS efficiency basically coincides with the PL intensity in this configuration.

When tilting the field by small angles only, for example $\theta = 10°$, considerable differences show up. For QD sample #1 with the strongest lateral confinement, the maxima of the two distributions still coincide over the whole magnetic field range studied. This is also true for the two other samples, but only at low fields. At high fields the maximum of the SFRS efficiency is shifted toward higher energies as compared to the PL maximum. This is shown in detail in Figs. 6(a) and 6(b) by the solid symbols, evidencing as well that this high-energy shift is stronger for the QD sample with smaller

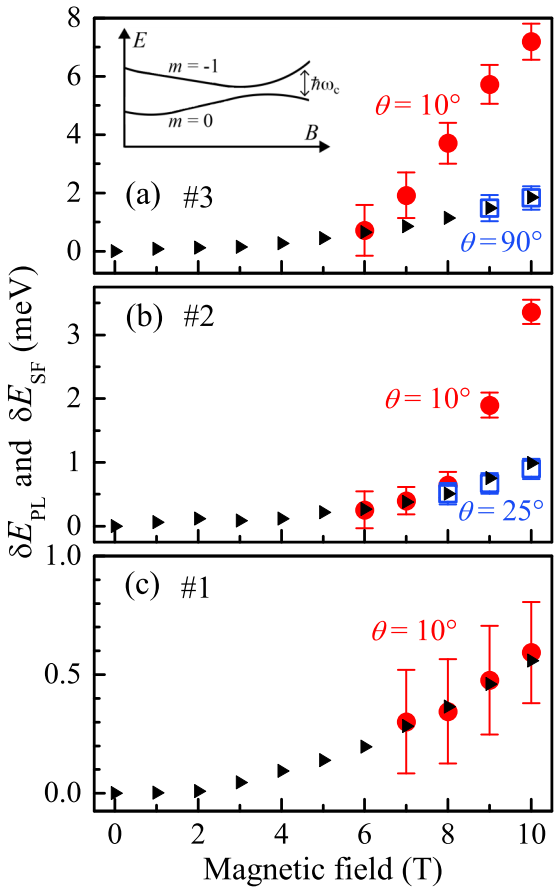

FIG. 6. (Color online) Magnetic field dependences of energy shifts for s-shell PL (triangles) and SFRS profiles (circles and squares) maxima measured for different geometries and the singly charged (In,Ga)As/GaAs QD samples. PL data of all samples are for $\theta = 10^\circ$. The uncertainty in δE_{SF} value primarily results from the width of the resonance profile. In the inset of panel (a), the anticrossing of the s- and p-shell states in tilted magnetic field is sketched.

lateral confinement as compared to the one with stronger confinement. The energy shift for the s-shell PL is denoted by δE_{PL} and that for the Raman profile by δE_{SF}, while the zero-energy value in the Figs. 6(a)–6(c) corresponds to the s-shell PL maximum at $B = 0$ T.

For all samples, the PL bands measured at small tilt angle $\theta = 10^\circ$ close to the Faraday geometry show weak diamagnetic shifts ($\propto B^2$) with increasing magnetic field, which are characteristic of confined exciton complexes. The diamagnetic shift, as expected, is larger for dots with larger in-plane size. In sample #1 with the smallest dots, the Raman profile and PL maxima at $\theta = 10^\circ$ coincide in the studied field range up to 10 T, see Fig. 6(c). In large-diameter dots, however, such a coincidence is fulfilled only below some threshold magnetic field, which is about 8 T for sample #2 and 6 T for sample #3. Above the threshold field a strong shift of the Raman profile maximum takes place, as demonstrated in Figs. 6(a) and 6(b). The difference to the PL maximum at $B = 10$ T reaches 5.3 meV in sample #3 and 2.3 meV in sample #2. It is interesting that such unexpected behavior is very sensitive to the magnitude of the tilting angle; in sample #2, e.g., it disappears for $\theta \geqslant 25^\circ$, see blue squares. The strong shifts can approximately be described by a linear dependence with a slope of (1.8 ± 0.1) meV/T, which is very much comparable with the cyclotron resonance energy $\hbar\omega_{\mathrm{c}} = \hbar eB/m_{\mathrm{e}}$ for an electron mass of $m_{\mathrm{e}} = (0.064 \mp 0.004)m_0$ with m_0 being the free electron mass. The mass is in agreement with the expected in-plane value for the electron in (In,Ga)As QDs [29,30].

Next, we have to clarify the origin of the high-energy shift of the e-SFRS efficiency whose maximum moves toward the excited state transition energies, compare the PL spectra in Fig. 1(a). Our data, however, also show that the excitation of higher lying states does not facilitate spin-flip scattering in general, as the respective scattering efficiency goes to zero, even though restrictions from the Pauli blocking do not exist for such transitions. This may be expected as the spin scattering is then no longer a resonant process but becomes off-resonant. Also, the lifetime of the excited states is shorter than that of the ground state which reduces the SFRS efficiency.

The observation that the shift starts at smaller magnetic fields for QDs with weaker in-plane confinement, which, in turn, corresponds to smaller QD-level splittings, suggests that the origin of the efficiency shift is a magnetic-field-induced state mixing in which the ground and first-excited states are involved. This state mixing becomes possible through the tilted field geometry by which terms proportional to $(e^2B^2/m_{\mathrm{e}})\sin(2\theta)xz$ appear in the single-particle Hamiltonian [31,32], where magnetic field components along the z and x axis are considered. Obviously the importance of these terms enhances strongly with magnetic field.

When the field is applied along the QD growth direction or in an oblique configuration with small tilt angle, the confined electron and hole orbital levels evolve in accordance to the Fock-Darwin (FD) spectrum [33]. The field component along the z axis leads to a splitting of states with positive and negative orbital angular momentum m. The first-excited state with $m = -1$ is most relevant for the mixing with the ground state of zero angular momentum. The splitting between these states is given by [34]

$$\Delta E = \hbar\sqrt{\omega_0^2 + \left(\frac{\omega_{\mathrm{c}}}{2}\right)^2} - \frac{1}{2}\hbar\omega_{\mathrm{c}}, \qquad (1)$$

where $\hbar\omega_0$ characterizes the lateral confinement energy of the electrons. It can be estimated from the splitting between the PL peaks as roughly 14 meV, 8.5 meV, and 6 meV for samples #1, #2, and #3, respectively. With increasing magnetic field the level splitting decreases, so that their mixing by the in-plane field component becomes significant, as stated in the previous paragraph. For very high magnetic fields (not reached in our studies) the levels converge to form Landau levels. The B field at which the mixing reaches relevance depends, however, on the quantum dot confinement. For the most strongly confining QDs it is apparently irrelevant, while it becomes the more important the less confining the dots are. Due to the mixing the levels repel each other, where the repulsion energy is determined by the mixing term given above, containing the cyclotron energy of the electrons, as observed in experiment. We suggest that it is this level mixing and repulsion, namely a hybridization of an s-shell and a p-shell state, which leads to the shift of the e-SFRS efficiency to higher energies starting from a magnetic field where the cyclotron energy is comparable

to the lateral confinement energy. This level anticrossing is sketched in the inset of Fig. 6(a). For the Voigt geometry, the separation between the ground state and the excited levels remains basically unchanged, so that the SFRS efficiency is also not altered.

For a complete, quantitative description, this single-particle discussion has to be extended by considering excitonic complexes. Accordingly, the SFRS efficiency shifts for the weakly confining QDs due to the hybridization of the s-shell trion singlet and p-shell trion triplet in slightly tilted magnetic field geometry. The observed Raman shifts correspond to pure spin-flips without involving relaxation between different quantum states or scattering between singlet and triplet spin configurations. Note that for ground-state excitation only the trion spin singlet can be excited, while for a laser energy tuned to the transition energy of the first-excited state, both trion spin triplets and singlet can be excited. For the p-shell trion, at zero magnetic field the spin singlet state is lying a few meV higher in energy than the triplet states [8]. In our tilted magnetic field geometry these spin states could also be mixed, which may be considered to describe the pure single electron-SFRS.

In conclusion, we have demonstrated that in singly charged (In,Ga)As/GaAs QDs after the resonant excitation of a negative trion the spin-flip scattering of the resident electron is realized by isotropic electron-electron exchange interaction. Anisotropic electron-hole exchange interaction and light-heavy-hole mixing, which is enhanced at higher excitation energies, lead to weakly efficient electron-SFRS in cross-circular polarization configurations. The major requirement for the allowance of the single spin-flip scattering process is the reduction of the trion symmetry by a magnetic field tilted with respect to the QD growth axis. The spin scattering based on isotropic exchange is much more efficient than the acoustic-phonon-mediated SFRS of the electron in the neutral exciton, whose Raman shift at $B = 0$ T corresponds to the exciton exchange energy δ_0. We have further shown that, when the magnetic confinement dominates against the lateral QD confinement above a threshold magnetic field, the maximum efficiency of the resident electron spin-flip scattering strongly shifts with increasing magnetic field, whereby the shift is described by the electron cyclotron energy. This surprising behavior is observed in large-diameter QDs and close-to-Faraday geometries. We have suggested as explanation that the s-shell singlet and p-shell triplet with $m = -1$ of the negative trion are hybridized, and the repulsion of their levels is defined by the electron cyclotron energy. On the whole, resonant SFRS is a promising experimental tool to investigate in detail spin-flip scattering mechanisms in low-dimensional semiconductor structures, particularly due to its sensitivity to the symmetry and type of the probed exciton complex.

We acknowledge R. A. Suris, I. A. Akimov, and A. Greilich for fruitful discussions. This work was supported by the Deutsche Forschungsgemeinschaft via SPP 1285 and the Mercator Research Center Ruhr (MERCUR) of Stiftung Mercator. The research stay of V.F.S. in Dortmund was supported by the Deutsche Forschungsgemeinschaft (Grant No. YA65/10-1). J.D. thanks the Rudolf-Chaudoire-Stiftung for financially supporting his research stay at the Ioffe institute. V.F.S. and M.B. acknowledge partial financial support from the Russian Ministry of Education and Science (Contract No. 14.Z50.31.0021). V.F.S. further acknowledges financial support from St. Petersburg State University (Grant No. 11.38.277.2014).

[1] A. G. Curto, G. Volpe, T. H. Taminiau, M. P. Kreuzer, R. Quidant, and N. F. van Hulst, Science **329**, 930 (2010).

[2] A. Kolli, B. W. Lovett, S. C. Benjamin, and T. M. Stace, Phys. Rev. Lett. **97**, 250504 (2006).

[3] H. Kosaka, T. Inagaki, Y. Rikitake, H. Imamura, Y. Mitsumori, and K. Edamatsu, Nature (London) **457**, 702 (2009).

[4] *Spin Physics in Semiconductors*, edited by M. Dyakonov (Springer, Berlin, 2008).

[5] A. Greilich, D. R. Yakovlev, A. Shabaev, Al. L. Efros, I. A. Yugova, R. Oulton, V. Stavarache, D. Reuter, A. Wieck, and M. Bayer, Science **313**, 341 (2006).

[6] D. Press, T. D. Ladd, B. Zhang, and Y. Yamamoto, Nature (London) **456**, 218 (2008).

[7] *Optical Generation and Control of Quantum Coherence in Semiconductor Nanostructures*, Springer Series in Nanoscience and Technology, edited by G. Slavcheva and Ph. Roussignol (Springer, Berlin, 2010).

[8] S. G. Carter, Ş. C. Bădescu, and A. S. Bracker, Phys. Rev. B **81**, 045305 (2010).

[9] Y. Igarashi, M. Shirane, Y. Ota, M. Nomura, N. Kumagai, S. Ohkouchi, A. Kirihara, S. Ishida, S. Iwamoto, S. Yorozu, and Y. Arakawa, Phys. Rev. B **81**, 245304 (2010).

[10] J. J. Finley, A. D. Ashmore, A. Lemaitre, D. J. Mowbray, M. S. Skolnick, I. E. Itskevich, P. A. Maksym, M. Hopkinson, and T. F. Krauss, Phys. Rev. B **63**, 073307 (2001).

[11] A. Greilich, M. Wiemann, F. G. G. Hernandez, D. R. Yakovlev, I. A. Yugova, M. Bayer, A. Shabaev, Al. L. Efros, D. Reuter, and A. D. Wieck, Phys. Rev. B **75**, 233301 (2007).

[12] M. Atatüre, J. Dreiser, A. Badolato, and A. Imamoglu, Nat. Phys. **3**, 101 (2007).

[13] J. Debus, D. Dunker, V. F. Sapega, D. R. Yakovlev, G. Karczewski, T. Wojtowicz, J. Kossut, and M. Bayer, Phys. Rev. B **87**, 205316 (2013).

[14] J. Puls, M. Rabe, H.-J. Wünsche, and F. Henneberger, Phys. Rev. B **60**, R16303(R) (1999).

[15] J. Debus, T. S. Shamirzaev, D. Dunker, V. F. Sapega, E. L. Ivchenko, D. R. Yakovlev, A. I. Toropov, and M. Bayer, Phys. Rev. B **90**, 125431 (2014).

[16] M. Yu. Petrov, I. V. Ignatiev, S. V. Poltavtsev, A. Greilich, A. Bauschulte, D. R. Yakovlev, and M. Bayer, Phys. Rev. B **78**, 045315 (2008).

[17] A. Greilich, D. R. Yakovlev, and M. Bayer, *Optical Generation and Control of Quantum Coherence in Semiconductor Nanostructures*, edited by G. Slavcheva and Ph. Roussignol (Springer, Berlin, 2010), Chap. 6, pp. 85–127.

[18] A. Greilich, M. Schwab, T. Berstermann, T. Auer, R. Oulton, D. R. Yakovlev, M. Bayer, V. Stavarache, D. Reuter, and A. Wieck, Phys. Rev. B **73**, 045323 (2006).

[19] I. A. Yugova, A. Greilich, E. A. Zhukov, D. R. Yakovlev, M. Bayer, D. Reuter, and A. D. Wieck, Phys. Rev. B **75**, 195325 (2007).
[20] A. Schwan, B.-M. Meiners, A. B. Henriques, A. D. B. Maia, A. A. Quivy, S. Spatzek, S. Varwig, D. R. Yakovlev, and M. Bayer, Appl. Phys. Lett. **98**, 233102 (2011).
[21] D. Richards and B. Jusserand, Phys. Rev. B **59**, R2506 (1999).
[22] The SFRS lines with very weak intensities, e.g., the e-SFRS for (σ^-, σ^+) in the anti-Stokes region, are due to a slight ellipticity of the polarization of the incident light introduced by the laser mirror used at the sample holder inside the magnet-cryostat.
[23] H. Kurtze, D. R. Yakovlev, D. Reuter, A. D. Wieck, and M. Bayer, Phys. Rev. B **85**, 195303 (2012).
[24] For the neutral exciton, the Raman shift is described by $\Delta E_{\mathrm{SF}} = \sqrt{\delta_0^2 + (\mu_{\mathrm{B}} g_{\mathrm{X}} B)^2}$ in Faraday and slightly tilted geometries.
[25] M. Dyakonov, X. Marie, T. Amand, P. Le Jeune, D. Robart, M. Brousseau, and J. Barrau, Phys. Rev. B **56**, 10412 (1997).
[26] L. M. Woods, T. L. Reinecke, and Y. Lyanda-Geller, Phys. Rev. B **66**, 161318(R) (2002).
[27] T. D. Krauss and F. W. Wise, Phys. Rev. Lett. **79**, 5102 (1997).
[28] A. A. Sirenko, V. I. Belitsky, T. Ruf, M. Cardona, A. I. Ekimov, and C. Trallero-Giner, Phys. Rev. B **58**, 2077 (1998).
[29] M. Grundmann, O. Stier, and D. Bimberg, Phys. Rev. B **52**, 11969 (1995).
[30] A. P. Zhou and W. D. Sheng, Eur. Phys. J. B **68**, 233 (2009).
[31] S. C. Lee, J. Y. Ryu, S. W. Kim, and C. S. Ting, Phys. Rev. B **62**, 5045 (2000).
[32] G. Marx and R. Kümmel, J. Phys.: Condens. Matter **3**, 8237 (1991).
[33] S. Raymond, S. Studenikin, A. Sachrajda, Z. Wasilewski, S. J. Cheng, W. Sheng, P. Hawrylak, A. Babinski, M. Potemski, G. Ortner, and M. Bayer, Phys. Rev. Lett. **92**, 187402 (2004).
[34] P. A. Maksym and T. Chakraborty, Phys. Rev. Lett. **65**, 108 (1990).